FATIGUE STRENGTH OF WOOD UNDER PULSATING TENSION-TORSION COMBINED LOADING

Yasutoshi Sasaki

Associate Professor
Graduate School of Bioagricultural Sciences
Nagoya University
Chikusa, 464-8601 Nagoya, Japan

and

Mariko Yamasaki

Research Associate
Graduate School of Engineering Science
Osaka University
Toyonaka, 560-8531 Osaka, Japan

(Received July 2001)

ABSTRACT

Fatigue strength of wood under cyclic tension-torsion combined loading was investigated experimentally. The material used for the experiments was a rectangular bar of Japanese cypress. Pulsating tension-torsion combined loadings were respectively applied along and around the longitudinal axis of the specimen, which coincided with the longitudinal direction of the wood. The obtained results of fatigue tests were found to be influenced by the combined-stress ratios and the applied stress levels, and were summarized as follows: 1) All data were located in a slightly wide band on the *S-N* plot in spite of different combined-stress ratios, but the slope of the *S-N* curves became low when tensile stress was dominant. 2) Failure modes of the test specimen depended on whether tensile or shear stress was dominant in the biaxial stress ratios. 3) Hill's criterion for the static strength was suitable for evaluating the fatigue strength under combined-stress ratios.

Keywords: Fatigue, combined loading, *S-N* curve, failure criterion, biaxial stress.

INTRODUCTION

It is rare for a component-member that constitutes a structure to be subjected to a simple stress state. Usually, it is subjected to a compound stress state in many cases. For the rational design of a structure, it is important to know the mechanical characteristics of the material under such a state. Many studies have been conducted to understand the mechanical behavior under combined stress of materials such as concrete, steel, FRP and bone (Cezayirlioglu et al. 1985; Fujii et al. 1992; Krempl and Niu 1982; Okajima 1970; Owen and Griffiths 1978).

On the other hand, there are many studies on the mechanical behavior in cases where a load, such as compression, tension, or bending, independently acts on wood or a wood-based material, statically or dynamically (Imayama and Matsumoto 1970; Okuyama et al. 1984; Suzuki and Saito 1984). However, there are few studies on the mechanical behavior under combined loading in which such loads act on those materials simultaneously (Origuchi et al. 1997; Yamasaki et al. 1999; Yamasaki and Sasaki 2000a, b, 2001a, b). There are no reported studies on the fatigue behavior under combined loading. This may be the reason for the small number of cases where wood is used under such a situation. However, the technical development of timber structures in recent years in engineering studies and construction has been significant. There is a need to understand the mechanical behavior of wood under combined loading not

Wood and Fiber Science, 34(4), 2002, pp. 508–515

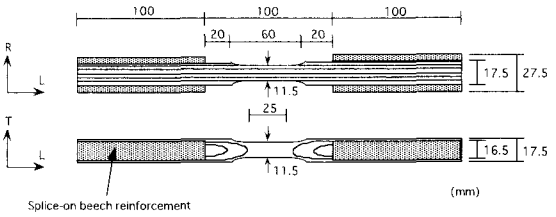

FIG. 1. Test specimen (Japanese cypress) used in this experiment. Japanese beech was spliced to reinforce grip-area using an epoxide resin adhesive and screws.

only in the case of uniaxial load but also in the case of torsion and axial loads acting simultaneously. Furthermore, wood is an organic material that exists naturally and has typical orthotropy similar to a bone. Therefore, it is expected that the information on the mechanical behavior of such material under combined stress is useful in the creation of a new composite material (Takahashi 1999).

With these points as the background, the mechanical behavior of wood under combined stress was investigated (Origuchi et al. 1997; Yamasaki et al. 1999; Yamasaki and Sasaki 2000a, b, 2001a, b). In this research, a rectangular bar of Japanese cypress was used as a test piece, and a fatigue test was performed under combined tension and torsion. It was aimed at investigating the fatigue strength characteristic of wood under combined loading. That is, this research focused, in particular, on the influence of the combined-stress ratio on the fatigue strength of Japanese cypress as the first step in the evaluation of the fatigue characteristics of wood under multiaxial stress.

MATERIAL AND METHODS

Specimen

Air-dried samples of Japanese cypress (*Chamaecyparis obtusa* Endl.) were tested. The specimen was cut to have a rectangular cross section with its major axis lying in the fiber direction, as shown in Fig. 1. The dimensions of the specimen were 300 mm (L) $\times$ 17.5 mm (T) $\times$ 17.5 mm (R). In the central part of the specimen, a taper was attached to four planes, and a portion with cross-sectional dimensions of 11.5 mm $\times$ 11.5 mm and length of more than 25 mm was prepared, as shown in Fig. 1. A firm grip was formed at the two ends by attaching spliced pieces of Japanese beech (*Fagus crenata* Bl.) using an epoxide resin adhesive and screws. The specimens were cured in the laboratory maintained at 25°C and a relative humidity of 40%, until the constant weights of specimens were achieved. The total number of specimens used was 120 in all tests, as shown in Table 1. They were selected based on specific gravity to minimize scatter in material quality among test groups shown in Table 1. The specific gravity and the moisture content were 0.44 $\pm$ 0.01 and 7.8 $\pm$ 0.3% in average of all specimens, respectively.

Test conditions and methods

In order to determine the static strengths used as the standard of a fatigue test, uniaxial loading and pure torsion tests, and static compression-torsion and tension-torsion combined

TABLE 1. *Number of specimens used in this experiment.*

Type of tests	Groups (Stress states)	Number of specimens	Remarks
Static tests	Pure tension	5	Results of the static tests were plotted in Fig. 2.
	Pure compression	5	
	Pure torsion	5	
	Combined tension-torsion	14	
	Combined compression-torsion	12	
Fatigue tests	Pure torsion: S	18	Two to five specimens were used for each stress level.
	Combined tension-torsion: TA	15	
	Combined tension-torsion: TB	15	
	Combined tension-torsion: TC	15	
	Pure tension: T	16	

loading tests were first carried out. An electro-hydraulic servo machine (EHF-ED 10/TD1-20L manufactured by Shimadzu Corporation, Kyoto) for the static loading tests was used. An axial force was applied in the fiber direction (along L) and torque was applied around an axis lying in the same direction as L. At the respective centers of a cross grain plane (LT plane) and a straight grain plane (LR plane), a triaxial rosette gage (KFG-3-120-D17 manufactured by Kyowa Electronic Instruments Co., Ltd., Tokyo, with gage length of 3 mm and 120 Ω) was attached. The applied axial force and torque, and the axial and rotational displacements were measured by load cells and electric displacement transducers on the testing machine itself, while the longitudinal and shear strains were also measured by strain gages on the LT and LR planes. All tests were carried out at 25°C and a relative humidity of 40%. The procedures for these static loading tests were as follows.

Uniaxial loading and pure torsion tests

In order to determine the static strengths in tension, compression, and torque, uniaxial loading and pure torsion tests were carried out under a controlled condition using a constant rate of displacement. The number of specimens for each test was five, as shown in Table 1. The axial force was applied at a constant axial displacement rate of 0.01 mm/s and the torque at a constant rotational rate of 0.05 deg/s.

Combined loading tests

In order to determine the failure surface, the combined loading tests were conducted by the proportional deformation loading method, in which the axial force and torque were applied simultaneously to the test specimen with their displacement rates kept constant. By changing the ratio of application rates of the axial displacement and rotation, a failure surface resulting from the combination of axial stress and shear stress at the time of failure was created. As loading was applied under a controlled condition using a constant rate of displacement, the displacement rate was set not to exceed 1.5 times the rate used in uniaxial loading and pure torsion tests so as to avoid the effect of impact forces. The number of specimens for these tests was 26, as shown in Table 1.

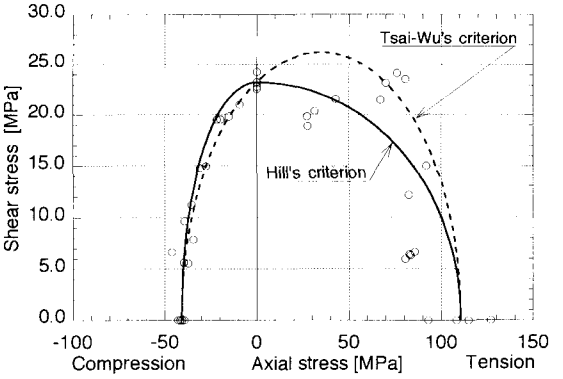

FIG. 2. Static strength under combined loading.

Figure 2 shows the results marked by circles (○) and the failure surface obtained by these static tests. The strength was determined by considering the anisotropy of wood (Origuchi et al. 1997; Suzuki and Okohira 1982; Yamasaki and Sasaki 2000a; Yoshihara and Ohta 1993). In the figure, two well-known failure criteria expressed by Eqs. (1) and (2), which established the failure condition, are also drawn. These equations were originally proposed by Hill, and Tsai and Wu, respectively (Hill 1948; Tsai and Wu 1971).

$$\left(\frac{\sigma_A}{F_A}\right)^2 + \left(\frac{\tau_S}{F_S}\right)^2 = 1 \quad (1)$$

$$\left(\frac{1}{F_{At}} - \frac{1}{F_{Ac}}\right)\sigma_A + \frac{1}{F_{At}F_{Ac}}\sigma_A{}^2 + \left(\frac{1}{F_S{}^2}\right)\tau_S{}^2 = 1 \quad (2)$$

where σ_A is the axial stress, τ_S is the shear stress, and F_A and F_S are the axial (tensile or compressive) strength and the shear strength, respectively. In Eq. (2), F_{At} and F_{Ac} are the uniaxial strengths in tension and compression, respectively. As shown in Fig. 2, both criteria are in good agreement to express the failure condition roughly.

In order to determine the combined-stress

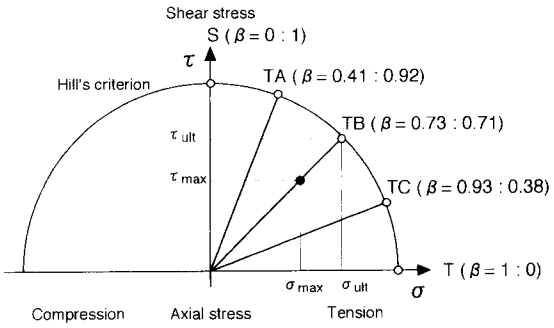

FIG. 3. Schema of Hill's criterion and combined stress ratios determined for fatigue tests.

ratios for fatigue tests under combined loading, Hill's criterion was chosen, while Tsai-Wu's criterion was more suitable, in part, to evaluate the combined-stress states where shear stress was applied dominantly. Because Tsai-Wu's criterion is located outside of Hill's criterion in the quadrant of tensile and shear stress, Tsai-Wu's criterion provides a more severe test condition for fatigue tests. Based on the standardized Hill's criterion for each static strength, the combined-stress ratios for the fatigue tests were determined, as schematically shown in Fig. 3—namely, the combined-stress ratio (β) of this study was defined by the ratio of axial stress to shear stress. Five ratios (β), that is, combinations of axial and shear stresses (indicated as S, TA, TB, TC, and T) were set up as follows: β = 0:1 (pure torsion, indicated as S), 0.41:0.92 (TA), 0.73:0.71 (TB), 0.93:0.38 (TC), and 1:0 (pure tension, T), and are shown in Table 2. These β ratios divided equally the quadrant of tension-shear combined-stress states into four based on the failure criterion shown in Fig. 3. Each number indicated the ratio of the stress to pure tensile or shear strength (σ_A/F_A or τ_S/F_S). As known by these ratios, shear stress component was dominant in the combined-stress state TA and tensile stress component in TC. In the TB state, shear and tensile stress components were almost equally applied. The values for each combination are shown in Table 2 and in Fig. 3.

Fatigue tests

The same testing machine used for static tests, which could apply axial and torsional loads simultaneously, was used for fatigue tests. A pulsating triangular axial load of tension was applied in the longitudinal direction at 1 Hz, while the specimen was also simultaneously subjected to a twisting moment, as illustrated in Fig. 4. The relationship between tensile stress and shear stress for a loading path is given by a straight line, as illustrated in Figs. 3 and 4. Stress levels in the fatigue tests were determined as the ratio of maximum stress to ultimate stress on the basis of the values shown in Table 2, and six stages equivalent to 100, 90, 80, 70, 60, and 50% of these values were determined as the stress levels. For each stress level, two to five specimens were used for fatigue tests. The total number of specimens for fatigue tests was 79, as shown in Table 1. They were selected based on specific gravity to minimize scatter in material quality among five test groups shown in Table 1.

The applied axial force and torque, and the axial and rotational displacements were mea-

TABLE 2. *Stress ratios and ultimate stresses in tension and shear.*

Combined-stress state	Combined-stress ratio (β)		Ultimate stress [MPa]		Remarks
	Axial	Shear	Axial (σ_{ult})	Shear (τ_{ult})	
S	0	1	0.00	23.5	Pure torsion
TA	0.41	0.92	45.1	21.6	
TB	0.73	0.71	81.3	16.7	Combined tension and shear
TC	0.93	0.38	103	8.82	
T	1	0	111	0.00	Pure tension

Each number of the combined-stress ratio (β) indicates the ratio of stress to pure tensile or pure shear strength, that is, σ_A/F_A or τ_S/F_S.

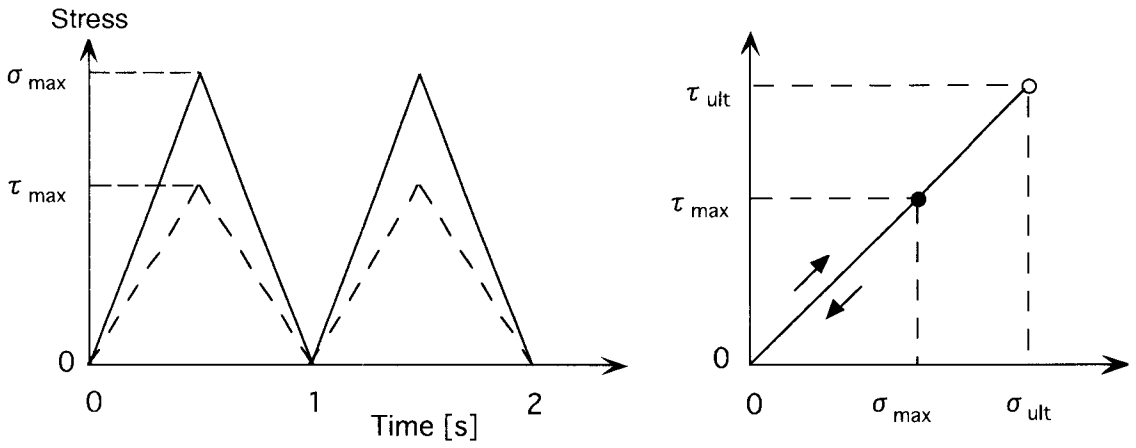

FIG. 4. Waveform and loading path for fatigue tests.

sured by load cells and electric displacement transducers on the testing machine itself, while the longitudinal and shear strains were also measured by strain gages on the LT and LR planes. All tests were carried out at 25°C and a relative humidity of 40%.

RESULTS AND DISCUSSION

Influence of combined-stress ratio on fatigue strength

Figure 5 shows the *S-N* curves obtained by fatigue tests. Horizontal and vertical axes show the fatigue life and the normalized maximum stress based on nominal stress (=stress level), respectively. The static strength data in pure torsion and pure tension are also included as part of the data for $Nf = 1$ (cycle) case. Each straight line in the figure is obtained by the least squares method, assuming that the life curves on a semilogarithmic plot are straight lines. From these, the *S-N* curve of each combined-stress ratio (β) could be deduced to collect into one thick strap, although a variation was observed. Based on these *S-N* curves, it appeared that the decreasing fatigue strength was caused by the combined-stress ratio. That is, the inclination of the *S-N* curve became large as the shear stress increased (TC → TB → TA) in the combined-stress state and was the largest when shear stress was applied dominantly (TA). Conversely, the inclination tended to decrease as the tensile stress increased. The *S-N* curve of S coincided almost with one of TA.

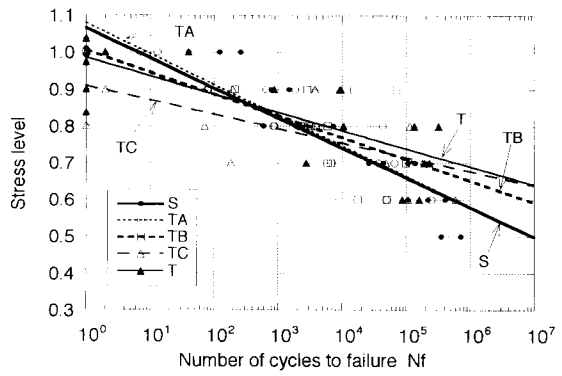

FIG. 5. Relationship between the stress ratio and the number of cycles to failure.

The above results on the *S-N* curves could also be considered as follows. When the stress level was higher than 85%, for example, the fatigue life of TA was the longest, and the fatigue life became short as the tensile stress increased (TA → TB → TC). However, when the stress level was reduced to 70%, the tendency was reversed. That is, the fatigue life became short as the torsion in the combined-stress ratio increased (TC → TB → TA). In addition, such a tendency is interesting because it is completely contrary to the results observed in other industrial materials. Fujii et

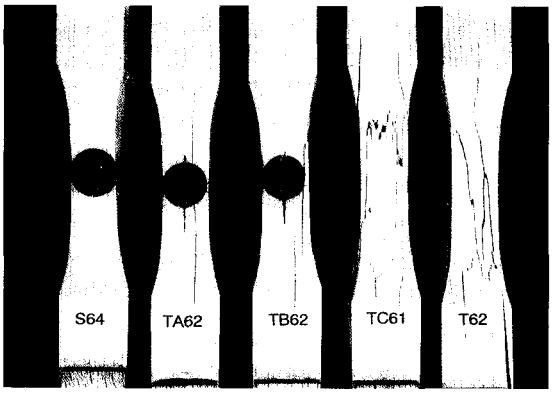

FIG. 6. Examples of failure modes by fatigue tests at a stress level of 60%. From left to right, typical failure modes under pure torsion (S), combined-stress (TA, TB, TC) and pure tension (T) states are shown.

al. conducted fatigue tests of a woven glass fabric composite under biaxial tension-torsion loading (Fujii et al. 1992). They found the tendency that the slope of the *S-N* curve became low in case of a high shear stress component could be distinguished. It is thought that this phenomenon is due to the organization structure of the material.

The regression lines of TA and S, for example, showed that the values for $Nf = 1$ were slightly larger than the static strength. Generally, the extrapolated value for $Nf = 1$, which was calculated from the linear regression of the fatigue results, did not agree with the static value (McNatt 1978). One of the reasons for this discrepancy was the difference in the loading rate between the static test and the fatigue test (McNatt 1970). Furthermore, it was considered that the fracture mechanism of the specimens in the fatigue test differed from that in the static test.

Influence of combined-stress ratio on failure mode

Figure 6 shows examples of the failure modes obtained by the fatigue tests performed under each combined-stress ratio. These examples, at a stress level of 60%, from left to right, show a pure torsion (S) state, combined-stress (TA, TB, TC) states, and a pure tension (T) state, respectively. Based on these examples, when the combined-stress ratio was in the S, TA, and TB states, a crack along the fiber was observed and torsion failure was considered to be dominant. On the other hand, in the TC state, combined failure of torsion and tension was observed, and typical tension failure was observed only in the T state. Thus, bordering on the TB state, torsion or tension failure became dominant, and the influence of the combined-stress ratio on the failure mode was identified. In addition, when the stress level was increased, the same destructive tendency as that shown in Fig. 6 was observed. However, the combined failure by torsion and tension was observed in the TB state. On the basis of the *S-N* curves in Fig. 5, this tendency appeared to be related to that of the fatigue life of TB becoming shorter than those of S and TA as the stress level was increased, though the experimental data at the stress level of 90% in Fig. 5 didn't show such a tendency. It was considered that the effect of tensile stress on failure became more serious at higher stress levels. In contrast, the effect of shear stress on failure became more serious at lower stress levels. In the TB state, where tensile and shear stresses were produced at equal levels, the failure at higher stress levels seemed to be influenced considerably by tension, and the combined failure by torsion and tension was observed. However, the failure at the stress level of 60% seemed to be influenced by torsion, and torsion failure became dominant, as shown in Fig. 6.

Fatigue strength and static failure criterion

The *S-N* characteristics were investigated on the tensile-shear stress ($\sigma - \tau$) plane—namely, the fatigue strength of each combined-stress state for $Nf = 10^3 - 10^6$ (cycles) was plotted on the $\sigma - \tau$ plane standardized by each static strength, as shown in Fig. 7. Points marked by black circles (●) were obtained from the *S-N* curves in Fig. 5. The outermost curve in the figure showed Hill's criterion, which was applied to static strengths (○). The other curves

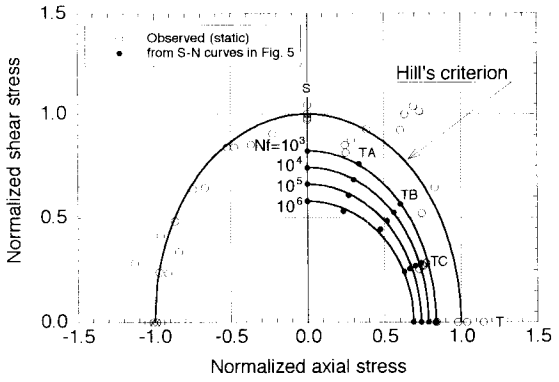

FIG. 7. Static and fatigue strengths under combined loading.

that were also obtained using Hill's Eq. (3), were determined from the fatigue strengths in uniaxial tension and pure shear obtained from the *S-N* curves labeled "T" and "S" in Fig. 5 for each fatigue life (*Nf*).

$$\left(\frac{\sigma_A}{F_A(Nf)}\right)^2 + \left(\frac{\tau_S}{F_S(Nf)}\right)^2 = 1 \qquad (3)$$

where σ_A is the axial stress, τ_S is the shear stress, and $F_A(Nf)$ and $F_S(Nf)$ are the axial (tensile or compressive) strength and the shear strength, respectively. Although Hill's equation was applied originally to static strengths, it was used here for fatigue strengths. These curves also expressed the envelope surfaces of the fatigue strengths for each fatigue life (*Nf*). As shown in Fig. 7, these surfaces seem to be in good agreement with each plot group of the combined-stress state. Therefore, the fatigue strength surfaces could be expressed by the static failure criterion. It was also considered that the fatigue strengths under arbitrary combined-stress states could be predicted by those in uniaxial tension and pure shear.

CONCLUSIONS

The results obtained are summarized as follows:

1) For decreasing fatigue strength, according to the *S-N* curve, the influence of combined-stress ratio was recognized. The inclination of the *S-N* curve became large as the shear stress component increased in the tension-shear combined-stress state.
2) As for the failure mode, torsional or tensile failure became dominant, bordering on the combined-stress state of TB, and the influence of combined-stress ratio (β) on the failure mode was observed.
3) Fatigue strength could be expressed approximately by Hill's criterion for static strength.

Further investigations are required to clarify the mechanical behavior of wood under combined-stress states.

REFERENCES

CEZAYIRLIOGLU, H., E. BAHNIUK, D. T. DAVY, AND K. G. HEIPLE. 1985. Anisotropic yield behavior of bone under combined axial force and torque. J. Biomech. 18:61–69.

FUJII, T., S. AMIJIMA, F. LIN, AND T. SAGAMI. 1992. Fatigue behavior of plain woven glass fiber laminates under pulsating tension/pulsating torsion combined loading (in Japanese). Trans. Jpn. Soc. Mech. Eng. (A) 58:1751–1758.

HILL, R. 1948. A theory of the yielding and plastic flow of anisotropic metals. Proc. Royal Soc. Series A 193: 281–297.

IMAYAMA, N., AND T. MATSUMOTO. 1970. Studies on the fatigue of wood—Phenomenal study on the fatigue process (in Japanese). J. Jpn. Wood Res. Soc. 16:319–325.

KREMPL, E., AND T. M. NIU. 1982. Graphite/Epoxy [±45]s tubes. Their static axial and shear properties and their fatigue behavior under completely reversed load controlled loading. J. Comp. Mat. 16:172–187.

MCNATT, J. D. 1970. Design stresses for hardboard—Effect rate, duration, and repeated loading. Forest Prod. J. 20:53–60.

———. 1978. Linear regression of fatigue data. Wood Sci. 11:39–41.

OKAJIMA, T. 1970. The strength of concrete under combined axial force (compression and tension) and torsional moment (in Japanese). Trans. Arch. Inst. Jpn. 178:1–9.

OKUYAMA, T., A. ITOH, AND S. N. MARSOEM. 1984. Mechanical responses of wood to repeated loading I—Tensile and compressive fatigue fractures. J. Jpn. Wood Res. Soc. 30:791–798.

ORIGUCHI, K., H. YOSHIHARA, AND M. OHTA. 1997. Yield behavior of wood under compression-shear combined stress condition (in Japanese). J. Soc. Mat. Sci. Jpn. 46: 385–389.

OWEN, M. J., AND M. J. GRIFFITHS. 1978. Evaluation of biaxial stress failure surfaces for a glass fabric rein-

forced polyester resin under static and fatigue loading. J. Mater. Sci. 13:1521–1537.

SUZUKI, N., AND Y. OKOHIRA. 1982. On the measurement of shearing strength by means of the torsion test of wood sticks with rectangular cross section (in Japanese). Bull. Fac. Agr. Mie Univ. 65:41–49.

SUZUKI, S., AND F. SAITO. 1984. Fatigue behavior of particle board in tension perpendicular to the surface—Effect of the surface. J. Jpn. Wood Res. Soc. 30:799–806.

TAKAHASHI, H. E. (ED.). 1999. Mechanical loading of bones and joints. Springer-Verlag, Tokyo, Japan.

TSAI, S. W., AND E. M. WU. 1971. General theory of strength for anisotropic materials. J. Comp. Mat. 5:58–80.

YAMASAKI, M., AND Y. SASAKI. 2000a. Failure behavior of wood (Japanese cypress) under combined axial force and torque—Effect of loading method and loading path (in Japanese). Trans. Jpn. Soc. Mech. Eng. (A) 66: 1612–1619.

———, AND ———. 2000b. Effect of loading method on the elastic properties of wood (Japanese cypress) under combined axial force and torque (in Japanese). Trans. Jpn. Soc. Mech. Eng. (A) 66:2144–2150.

———, AND ———. 2001a. Yield behavior of wood under combined static axial force and torque. Exp. Mech. (received for publication)

———, AND ———. 2001b. Elastic properties of wood under combined static axial force and torque. J. Mater. Sci. (received for publication)

———, ———, AND K. ANDO. 1999. Mechanical properties of wood under combined axial force and torque (in Japanese). J. Jpn. Wood Res. Soc. 45:297–305.

YOSHIHARA, H., AND M. OHTA. 1993. Measurement of the shear moduli of wood by the torsion of a rectangular bar. J. Jpn. Wood Res. Soc. 39:993–997.